CHAPTER II
BACKGROUND AND LITERATURE SURVEY

2.1 Hydrogen

Hydrogen is a fascinating energy carrier. It can be produced from electricity and water. Its conversion to heat or power is simple and clean. When combusted with oxygen, hydrogen forms water. No pollutants are generated or emitted. The water is returned to nature where it originally came from. But hydrogen, the most common chemical element on the planet, does not exist in nature in its pure form. It has to be separated from chemical compounds, by electrolysis from water or by chemical processes from hydrocarbons or other hydrogen carriers.
(http://www.hyweb.de/NEWS/ Bossel-Eliasson_2003_Hydrogen-Economy.pdf)

2.2 Hydrogen Storage

Hydrogen storage is a materials science challenge because, for all four storage methods currently being investigated, materials with either a strong interaction with hydrogen or without any reaction are needed. Besides conventional storage methods, i.e. high pressure gas cylinders and liquid hydrogen, the physisorption of hydrogen on materials with a high specific surface area, hydrogen intercalation in metals and complex hydrides.

2.2.1 Compressed Hydrogen Gas

Most compressed hydrogen tanks operate at ambient temperatures and store the gas at pressures of 5,000 to 10,000 psi. Compressed hydrogen tanks are available from many manufactures and have been certified by standard agencies worldwide. They are used in on-board fuel cell vehicles, in portable and on-site power generators, and in interruptible power supply system, where fuel cells replace batteries. However, the conventional steel tanks are too heavy for hydrogen storage used for on-board vehicles, especially when made of premium steel to prevent metal

fatigue and leakage. Difficulty to control pressure is another drawback of using this method to store hydrogen (Busby, 2005).

2.2.2 Liquid Hydrogen Storage

Hydrogen liquefies at supercold (cryogenic) temperature (-253°C). Liquid hydrogen has a higher energy density than the compressed form, so a tank containing the same amount of fuel is smaller. For a given volume of fuel, liquid hydrogen would boost the driving range of a vehicle, allowing roughly two or three times the distance of a compressed gas tank, making the liquid form ideal for long road trips. Also, liquefied hydrogen tanks are not highly pressurized and can be filled-up faster than compressed gas tanks.

However, liquefaction requires much more work than compression, consuming at least 30 to 35% of hydrogen's energy content, or 11 to 12 kWh of electricity per kilogram of liquefied hydrogen. Also, cryogenic tanks require insulation and other special materials (Busby, 2005).

2.2.3 Solid-state Storage

Solid-state storage refers to the storage of hydrogen in metal hydrides, in chemical storage materials, and in nano-structured materials. This method of hydrogen storage offers perhaps the best opportunities for meeting the requirements for on-board storage. In these materials, hydrogen can be stored both reversibly and irreversibly. Reversible storage means that hydrogen is released by raising the temperature. For example, a metal hydride at a suitable pressure; hydrogen is subsequently replaced (stored) through the control of temperature and hydrogen pressure. Although temperature and pressure are the two typically controlled thermodynamic parameters, other types of energy (e.g., mechanical and acoustical) can be employed to control both the release and uptake of hydrogen. Ideally, storage and release of hydrogen should take place at temperatures between 0°C and 100°C and pressures of 1–10 bar and on time scales suitable for transportation applications (http://www.sc.doe.gov/bes/hydrogen.pdf).

2.2.4 Storage via Chemical Reactions

Hydrogen can be generated by reacting metals and chemical compounds with water. The common experiment, seen in many chemistry classes, where a piece of Na floating on water produces hydrogen, demonstrates the process. The Na transforms to NaOH in this reaction. The reaction is not directly reversible, but NaOH can be removed and reduced in a solar furnace back to metallic Na. Two Na atoms react with two H_2O molecules and produce one hydrogen molecule. The hydrogen molecule produces a H_2O molecule in combustion, which can be recycled to generate more hydrogen gas (Züttel, 2003).

2.3 Metal Hydrides and Complex Hydrides Materials

The materials for solid-state hydrogen storage have been nearly exclusively metals and metallic alloys, in which the metal matrix is expanded and filled with absorbed hydrogen atoms that are usually located in tetrahedral or octahedral interstitial sites. Atomic hydrogen stored in these interstitial sites recombines at particle surfaces to form molecular hydrogen upon release. A major emphasis of materials-related research has been to encapsulate hydrogen. Capacities exceeding two hydrogen atoms per metal atom have been demonstrated by using this approach. Most metal matrices investigated to date, however, consist of relatively heavy elements, and gravimetric storage capacities usually do not exceed 2 wt% H_2 when transition metals are major components (http://www.sc.doe.gov/bes/hydrogen.pdf).

Figure 2.1 is a van't Hoff diagram showing the dissociation pressures and temperatures of a number of hydrides. Light elements, such as Mg, have shown promising levels of stored hydrogen (3–7 wt% hydrogen), but they release hydrogen at high temperature (315°C at 1atm) (Sandrock, 1999). Although improvements in the kinetics of magnesium-based alloys have been achieved by nano-structuring and adding catalysts (Oelerich *et al.*, 2001; Barkhordarian *et al.*, 2003), the thermodynamics remain virtually unchanged (i.e., rather modest shifts in plateau pressures/van't Hoff lines). In comparison, $NaAlH_4$, a low-temperature (LT) hydride, and Na_3AlH_6, a medium-temperature (MT) hydride, offer promise for lowering the

hydrogen released temperature while attaining high storage capacity (above 5 wt%) by using both phases to provide hydrogen (http://www.sc.doe.gov/bes/hydrogen.pdf).

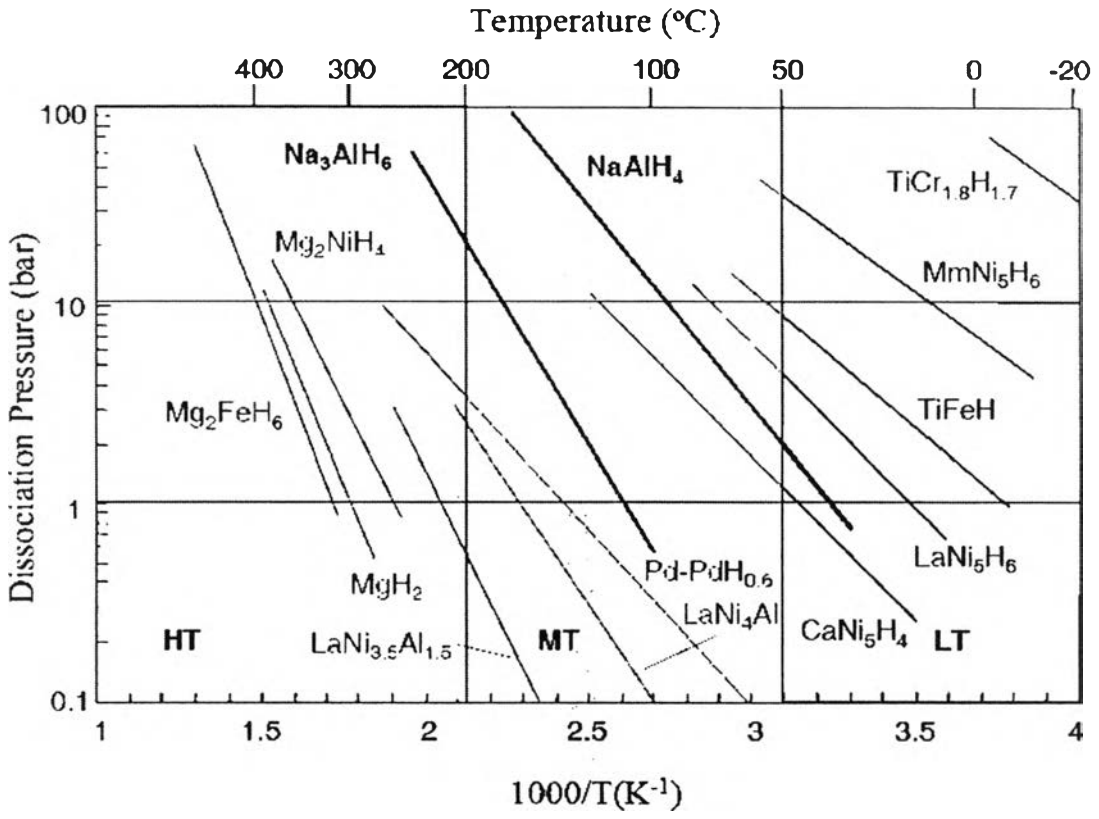

Figure 2.1 Van't Hoff diagram showing dissociation pressures and temperatures of various hydrides (http://www.sc.doe.gov/bes/hydrogen.pdf).

The reaction of hydrogen with a metal can be written as

$$M + x/2H_2 \leftrightarrow MH_x + \text{heat} \qquad (2.1)$$

where M = metal elements, and x = number of desorbed/absorbed hydrogen. Whether hydrogen is released or absorbed depends on the value of the Gibbs energy at the reaction conditions.

$$\Delta G = \Delta H - T\Delta S \qquad (2.2)$$

Hydrogen is absorbed if ΔG is less than zero and desorbed if ΔG is greater than zero.

Absorption and desorption are two steps involved to store hydrogen in metal hydrides. Energy is needed for the operation. The total energy required to operate a metal hydride storage system is about 12.5% of the low heating value of hydrogen and it is the lowest operating energy (Heung, 2003).

Metal hydrogen system consists of a H_2 gas, interface region and solid metal as shown in Figure 2.2. At the interface, the molecule is dissociated and dissolves into the metal phase.

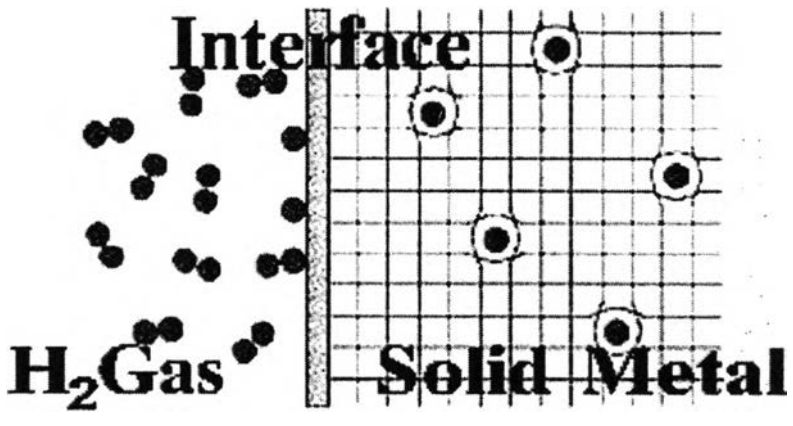

Figure 2.2 Model of the metal hydrides interaction (http://www.ovonic-hydrogen.com/solutions/technology1.htm).

The stages that are of interest are physisorption and chemisorption. The interaction of hydrogen molecule and metal surface in the physisorbed state is Van der Waals force. The physisorption energy is about 10 kJ/mol. When hydrogen is close to the surface, the hydrogen has to overcome an activation barrier of dissociation and the energy of the activation barrier depends on the surface elements. The hydrogen metal bond is formed. Hydrogen atoms share their electrons with the metal atoms in the chemisorbed state. The chemisorption energy is about 50 kJ/mol-H. The chemisorbed hydrogen atoms have high surface mobility, interact with each other, and form surface phases at high coverage (Züttel, 2003). The next stage, the chemisorbed hydrogen atom diffuses on the interstitial sites of the host metal lattice. Figure 2.3 shows a simplified one-dimensional potential energy curve.

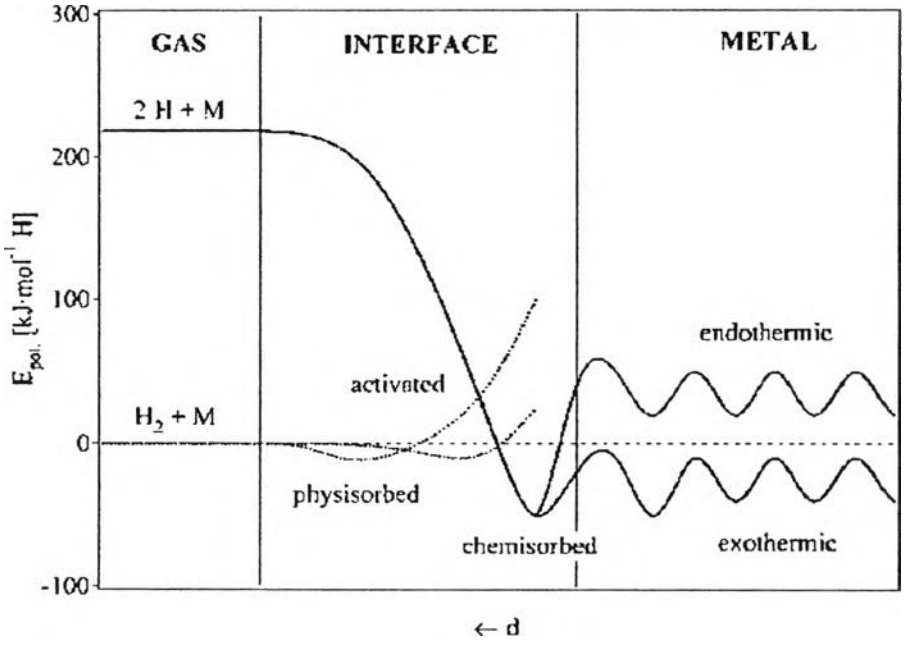

Figure 2.3 The potential energy of a hydrogen molecule and of two hydrogen atoms. The hydrogen molecule approaches to the metal atom by Van der Waals forces and forms a physisorbed state. Before diffusion into the metal, the hydrogen molecule has to overcome the activation barrier and dissociates to form a chemisorbed state (Züttel, 2003).

Some hydrogen is dissolved in the host metal as a solid solution. The hydrogen pressure increases proportional to the hydrogen concentration and the hydride phase occurs. In both of the solid solution and hydride phase region ($\alpha + \beta$ phase), the pressure change is small and size of the region depends on the hydrogen absorbed. Increasing hydrogen concentration until the phase completely changes to the pure hydride phase, the hydrogen pressure increases rapidly again (Schlapbach and Züttel, 2001). The hydrogen absorption on metal is represented by a PCT diagram as shown in Figure 2.4.

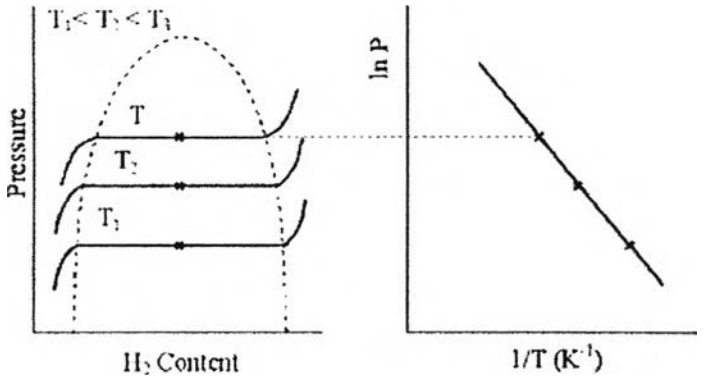

Figure 2.4 Pressure-concentration-temperature curve (PCT diagram) and Van't Hoff plot (Logarithm of the equilibrium against the reciprocal temperature) (http://www.ovonic-hydrogen.com/solutions/technology1.htm).

The hydrogen pressure that is in equilibrium depends on temperature and it is defined by the Van't Hoff equation:

$$\ln P = \frac{\Delta H}{RT} - \frac{\Delta S}{R} \qquad (2.3)$$

where ΔH and ΔS are the enthalpy and the entropy of the reaction, respectively, R is the gas constant and T is the temperature. The logarithm of pressure and one over temperature (lnP vs 1/T) are plotted, called Van't Hoff plot, Figure 2.4. The slope of the plot is related to the enthalpy of formation and the intercept is related to the entropy of formation. The enthalpy term gives the information about the stability of the metal hydrogen bond and the entropy term gives the information about hydrogen gas molecule to dissolved solid hydrogen.

Hydride formation in nearly all metal systems generally involves about a 15–25% volume change that must be accommodated in storage vessel designs. Another issue that needs to be addressed is the thermal management of the heats of absorption and desorption to (1) enhance the kinetics during filling and discharge of the hydrogen storage systems and (2) avoid degradation effects during long-life operation (http://www.sc.doe.gov/bes/hydrogen.pdf).

Table 2.1 Hydrogen storage capacities of hydrides

Hydride	Hydrogen (wt%)[a]
$NaAlH_4$	7.5
$LiAlH_4$	10.6
$Mg(AlH_4)_2$	9.3
$NaBH_4$	10.7
$LiBH_4$	18.5
$Mg(BH_4)_2$	14.9

[a]Note that these are theoretical total hydrogen contents and not reversible hydrogen capacities (Sandrock, 1999).

A different concept in solid-state storage of hydrogen is to encapsulate by hydrogen, thus opening the possibility of approaching the hydrogen content of methane. In some ways, CH_4 would seem to be the ultimate hydrogen storage compound, in which four hydrogen atoms surround a single carbon atom. However, because CH_4 is gaseous, it offers little practical benefit over storage of hydrogen itself. Further, the hydrogen-carbon bonds of methane are too strong for easy hydrogen recovery. Novel solids—such as alanates (aluminumhydrides), borohydrides, and imides—in which the metal atom is surrounded by four to six hydrogen atoms forming a complex negatively charged anion, mimic the structure of methane and may provide a much-needed breakthrough in the solid-state storage of hydrogen. As shown in Table 2.1, their theoretical total hydrogen capacities are high (from ~7 to 18 wt%).

Solid storage materials with a high volumetric density of hydrogen (up to 100 g H_2/L) would exceed the density of a cryogenic liquid at 20 K (~70 g H_2/L). The sidebar on light hydrides compares the mass density and volume density of hydrogen for a number of hydrides. Use of these materials is critically dependent on whether (and how) the stored hydrogen can be conveniently released at a temperature that is within acceptable bounds and how the materials can be recharged with hydrogen. Mixing hydrides to make complex, multicomponent hydrides could potentially allow the synthesis of storage materials with specifically tailored

properties. For example, the ionic bonding of hydrogen-rich $[MH_n]^{p-}$ anions with various light-element cations provides a means for precise chemical substitutions in the cation sublattice, thus bridging the gap between hydrogen-poor intermetallic hydrides and hydrogen-rich LiH, BeH_2, and MgH_2 compounds. Thus, these complex hydrides have perhaps the greatest potential to provide both a high wt% hydrogen and desirable release/absorption kinetics. Reaching the potential of hydrogen storage in these complex hydrides will require fundamental research in a number of areas, as outlined in the following sections (http://www.sc.doe.gov/bes/hydrogen.pdf).

2.3.1 Dopants

One of the most important, but least understood, findings is the critical role of dopants in achieving reasonable kinetics and reversibility of complex hydrides. For example, the addition of Ti-based compounds (such as $TiCl_3$ or $Ti[OBu]_4$ to $NaAlH_4$) was found to lower the first decomposition temperature of the hydride, so that 3.7 wt% is released at 80°C, but at the expense of lowering the hydrogen content from 5.5 wt% in the hydride without a catalyst (http://www.sc.doe.gov/bes/hydrogen.pdf).

2.3.2 Nano-scale Hydrides

Studies regarding the benefits of nano-scale versions of hydride materials relative to their bulk counterparts should be undertaken over the wide range of potentially interesting hydride materials for hydrogen storage. Theoretical guidance for designing potentially interesting nano-scale hydride materials should be used (Oelerich *et al.*, 2001).

2.3.3 Alkali Metal Hydrides

Light weight metal hydrides or alkali metal hydrides are divided into two parts: simple metal hydrides such as NaH, CaH_2, and LiH, and complex metal hydrides are group I and II salts of $[AlH_4]^-$, $[NH_2]^-$, and $[BH_4]^-$ (alanates, amides, and borohydrides) such as $NaAlH_4$, $LiAlH_4$, and $LiBH_4$. Hydrogen is covalently bonded to the central atoms in complex anions (in contrast to interstitial hydrides). Some examples and their properties are shown in Table 2.2.

Table 2.2 Examples of alkali metal hydrides and their properties

Material	Practical wt%	Kinetic reversibility	Desorption temperature (°C)	Notes
NaH	4.2	good	425	Low wt%, High temperature desorption
$NaAlH_4$	5.5	good	125	Not reach 6.5 wt%
$LiBH_4$	19.6	irreversible	380	Too stable
$LiH/LiNH_2$*	5.5	good	150-250	Not reach 6.5 wt%

(*$LiH/LiNH_2$ with $TiCl_3$)

(Grochala and Edwards, 2004)

2.3.4 Inter-Metallic Metal Hydrides

Inter-metallic metal hydrides can perform several functions: (1) enhancing the hydriding-dehydriding kinetic characteristic by acting like a catalyst, (2) altering the equilibrium pressure of the hydrogen absorption-desorption process to a desired level, and (3) increasing the stability of the alloy and preventing dissolution or formation of a compact oxide layer. They consist of two or more metals, which are alloyed together to form new chemical compounds. The compounds are a combination of element A, with a high ability to absorb hydrogen,

and element B, with a low ability to absorb hydrogen. Some families of inter-metallic compounds are listed in Table 2.3.

Table 2.3 Examples of inter-metallic compounds

Maximum Hydrogen Capacity				
Type	Intermetallic	H/M[a]	wt%	Temperature (°C) for 1 atm $P_{desorption}$
A_2B	Mg_2Ni	1.33	3.6	255
AB	TiFe	0.975	1.86	−10
AB	ZrNi	1.4	1.85	292
AB_2	$ZrMn_2$	1.2	1.77	167
AB_5	$LaNi_5$	1.08	1.49	12
AB_2	$TiV_{0.62}Mn_{1.5}$	1.14	2.15	−6

[a] H/M is the hydrogen-to-metal atomic ratio in the compound (Sandrock, 1999)

2.4 Comparison of Material's Hydrogen Storage Densities

Candidate materials for hydrogen storage will need to have high hydrogen packing density, as well as low weight. This sidebar compares these two properties —the mass density and volume density of hydrogen—for a number of different hydrogen-containing materials. The hydrogen density in the materials is simply proportional to the material density through the mass fraction. Three straightline plots are shown in Figure 2.5 for 5, 1, and 0.5 gm/cm^3. The best materials for hydrogen storage applications should be in the upper-right quadrant of the figure. Inter-metallic hydrides, such as $LaNi_5H_6$, have high volumetric densities, but generally are heavy—with specific gravities in the range of 5–10 gm/cm^3. They tend to populate the left-hand portion of Figure 2.5. Lighter compounds, with specific gravities of ~1 gm/cm^3, need to have high hydrogen-to-metal ratios to achieve high volumetric density. Some examples with high hydrogen content are shown in the

chart. Note that the hydrogen densities in solids tend to be comparable to the densities of hydrogen in hydrocarbon fuels, alcohols, and ammonia (http://www.sc.doe.gov/bes/hydrogen.pdf).

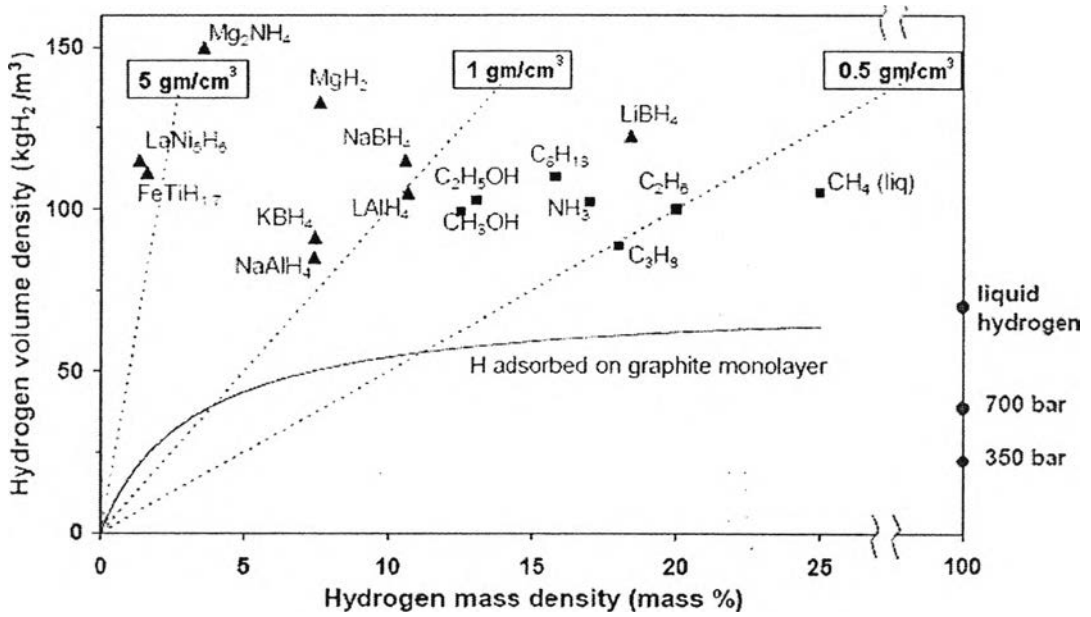

Figure 2.5 Comparison of metal hydrides, carbon nanotubes, petrol and other hydrocarbons. (Storing in hydrogen per mass and per volume).
(Schlapbach and Zuttel, 2001)

2.5 Li–N–H System

The Li-N-H system has high hydrogen-absorption potential (percentage of desorption hydrogen is 6.5 wt%) and its weight is quite low. However, it requires a high temperature for dehydrogenation and a high pressure for rehydriding. The reaction is as follows:

$$LiNH_2 + LiH \leftrightarrow Li_2NH + H_2 \qquad (2.4)$$

The assumption of suitable elementary reactions for Reaction (2.4) is as follows:

$$2LiNH_2 \rightarrow Li_2NH + NH_3 \qquad (2.5)$$

$$LiH + NH_3 \rightarrow LiNH_2 + H_2 \quad (2.6)$$

where, the enthalpy change of Reactions (2.5) and (2.6) could be calculated at +84 kJ/mol NH_3 and −42 kJ/mol H_2, respectively. For the acceleration of this reaction, the ball milling treatment was performed (Ichikawa *et al.*, 2005).

Chen *et al.* (2003) studied the interaction between lithium amide ($LiNH_2$) and lithium hydride (LiH). They demonstrated that pure $LiNH_2$ decomposed to litium imide (Li_2NH) and ammonia (NH_3) at temperature above 300°C. LiH, on the other hand, liberated hydrogen at temperature 550°C. When mixing these two substances and conducting temperature-programmed desorption (TPD), they noticed that hydrogen was produced at temperature around 150°C. Combined thermogravimetric (TG), x-ray diffraction (XRD), and infrared (IR) analysis revealed that $LiNH_2$ would react with LiH and convert to hydrogen and Li_2NH (or Li-rich imide).

Chen *et al.* (2007) reviewed the metal–N–H systems for the hydrogen storage. Hydrogen desorption from $LiNH_2$–2LiH and $LiNH_2$–LiH is a highly endothermic process with heat desorption of 80 and 66 kJ/mol H_2, respectively, and the operation temperature at 1.0 bar is above 250°C. In addition, it has also been reported that $TiCl_3$ and Li_2O can improve the kinetic of hydrogenation and dehydrogenation.

Hu and Ruckenstein (2003a) investigated hydrogen storage in Li_3N via temperature-programmed hydrogenation (TPH) and temperature-programmed dehydrogenation (TPD). They revealed that the TPH spectra indicated an initial hydrogenation temperature of Li_3N of ~ 150°C and increasing in hydrogen partial pressure accelerated the hydrogenation rate. The TPD curves exhibited three hydrogen peaks located at 240, 270, and above 380°C and the maximum amount of released hydrogen at low temperature was 6.0 wt%. XRD indicated that most of the low temperature released hydrogen can be attributed to the transformation of $LiNH_2$ to Li_2NH. Moreover, the amount and properties of the releasable hydrogen are also dependent on the duration and temperature of the Li_3N hydrogenation.

Hu and Ruckenstein (2003b) studied the reaction rate between LiH and NH_3 during hydrogen storage in Li_3N using the temperature-programmed decomposition of a two-layered of $LiNH_2$ and LiH. They demonstrated that NH_3 produced via the decomposition of $LiNH_2$ was completely captured by LiH even at very short contact times (25 ms) with the carrier gas. This ultrafast reaction between NH_3 and LiH inhibited NH_3 formation during the dehydrogenation of Li_3N and also prevented the NH_3 generated during the dehydrogenation of the hydrogenated Li_3N to escape into the hydrogen stream. However, if the hydrogenated Li_3N was previously exposed to atmosphere, some NH_3 could escape into the hydrogen stream during the hydrogen desorption, due to the partial oxidation of LiH by the water present in air.

Hu and Ruckenstein (2005) studied the reversibility of $LiNH_2/Li_3N$ mixtures. It was shown that the addition of $LiNH_2$ to Li_3N constitutes is an effective method to increase the reversible hydrogen capacity. They found that the reversible hydrogen capacity of the $LiNH_2/Li_3N$ mixture depends on its composition. A maximum reversible hydrogen capacity of 6.8 wt% could be achieved when the pre-added $LiNH_2$ content in the $LiNH_2/Li_3N$ mixture was between 28 and 50 mol%.

Ichikawa *et al.* (2004) studied reactions of 1:1 molar mixture of $LiNH_2$, and LiH. Without catalysts, the thermal desorption mass spectra indicated that hydrogen is released in the temperature range of 180 to 400°C and NH_3 is desorbed. However, the reaction can desorb 5.5 wt% hydrogen by using 1 mol% $TiCl_3$ as a catalyst from 150 to 250°C, and it does not desorb NH_3.

Isobe *et al.* (2005) studied the effect of Ti catalyst with different chemical form on Li-N-H hydrogen storage properties. The results indicated that the Ti^{nano}, $TiCl_3$ and TiO_2^{nano} doped composites revealed a superior catalytic effect on thermal hydrogen desorption spectrum (TDS) properties, while the Ti^{micro} and TiO_2^{micro} did not show good catalytic effect being similar to the sample without any additives.

Leng *et al.* (2008) investigated the reaction between $LiNH_2$ and hydrogen. They found that $LiNH_2$ can be converted to LiH and NH_3 by reacting with hydrogen under a hydrogen flow condition, while $LiNH_2$ is converted to Li_2NH and NH_3 by decomposition under Ar flow. Moreover, the reaction between $LiNH_2$ and hydrogen can be accelerated by mixing $LiNH_2$ with LiH as well as doping with $TiCl_3$.

Pinkerton (2005) studied the kinetic behavior of $LiNH_2$ decomposition for hydrogen storage. $LiNH_2$ is a primary component of the hydride state in Li-N-H storage materials based on Li_3N or Li_2NH. It was obtained by ball milling for 10 or 20 min and was detected by using thermo-gravimetric analysis (TGA). The reaction rate was found to depend on the sample size, as large samples produce a high concentration of NH_3.

Shaw *et al.* (2008) investigated the reaction pathway and rate-limiting step of dehydrogenation of the $LiNH_2$ + LiH mixture. They revealed that dehydrogenation of the $LiNH_2$ + LiH mixture was diffusion-controlled and rate-limiting step was identified to be diffusion of NH_3 through the porous Li_2NH product layer outside the $LiNH_2$ shrinking core. Moreover, their experiments revealed that nanocrystalline LiH and $LiNH_2$ particles generated via high-energy ball milling exhibited little or no growth in nanocrystalline sizes after 10 hydrogen soak/release cycles at 285 for 35 h. However, the surface area of the $LiNH_2$ + LiH powder mixture was decreased, indicating that an increasing in particle agglomeration during isothermal cycling.

2.6 Li–Al–H System

Lithium alanate or lithium aluminum hydride ($LiAlH_4$) has high hydrogen capacity for complete decomposition (7.9 wt%). It has multiple steps for decomposition

$$3LiAlH_4 \rightarrow Li_3AlH_6 + 2Al + 3H_2 \qquad (2.7)$$

$$Li_3AlH_6 \rightarrow 3LiH + Al + \frac{3}{2}H_2 \qquad (2.8)$$

The first step, Reaction (2.7), takes place at 160°C and releases 5.3 wt% hydrogen. The second step, Reaction (2.8), releases 2.6 wt% hydrogen and occurs at about 200°C. The unreleased part as LiH can be decomposed at very high temperature, above 680°C (Zaluski *et al.*, 1999).

Balema *et al.* (1999) studied the solid state phase transformations in $LiAlH_4$ during high-energy ball-milling. They revealed that good stability of this complex aluminohydride during high-energy ball-milling in a helium atmosphere and Li_3AlH_6 can be obtained from LiH and $LiAlH_4$ via solid state reaction. The decomposition of $LiAlH_4$ into Li_3AlH_6, Al, and H_2 was observed during mechanochemical for up to 110 h, and is most likely associated with the catalytic effect of the vial material.

Easton *et al.* (2005) studied factors affecting hydrogen released from $LiAlH_4$. They concluded that the mechanical milling of $LiAlH_4$ with $TiCl_3$ reduces the temperature for the thermal decomposition of $LiAlH_4$ and Li_3AlH_6. It is likely that the decomposition of $LiAlH_4$ into Li_3AlH_6 during the milling with $TiCl_3$ occurs not by mechanochemical decomposition, but rather because of a reduction of the decomposition temperature to room temperature or below.

2.7 Mg–N–H System

The Mg–N–H system has relatively mild thermodynamics. Hydrogen desorption from $Mg(NH_2)_2$ and MgH_2 at either a 1:1 or 1:2 molar ratio, Reactions (2.9) and (2.10) can occur under a mechanochemical reaction condition.

$$Mg(NH_2)_2 + MgH_2 \rightarrow 2MgNH + H_2 \qquad (2.9)$$

$$Mg(NH_2)_2 + 2MgH_2 \rightarrow Mg_3N_2 + 4H_2 \qquad (2.10)$$

Hydrogen evolved from the $Mg(NH_2)_2$–$2MgH_2$ mixture shortly after the ball milling, and desorption was accelerated after the mixture was ball milled for 5 h. The hydrogen release rate slowed down after about 20 h of milling. $Mg(NH_2)_2$ and MgH_2 are stable in the milling jar if ball milled alone. As expected, the solid residue is Mg_3N_2. Thermodynamic analysis revealed that the average heat of desorption is 3.5 kJ/mol H_2 for Reaction (2.10), indicating that Mg_3N_2 can hardly be converted to $Mg(NH_2)_2$ and MgH_2 under normal hydrogenation conditions. It took 72 h to complete the hydrogen desorption even if the dehydrogenation was allowed

thermodynamically. Therefore, the overall kinetics for hydrogen desorption should be rather slow, which might be the reason why investigations by other researchers have failed to detect the reaction between $Mg(NH_2)_2$ and MgH_2 (Chen *et al.*, 2007).

Hu *et al.* (2006) studied the effects of ball-milling conditions on dehydrogenation of $Mg(NH_2)_2$–MgH_2. The results reported that hydrogen gas released at temperature as low as 65°C, while the decomposition of $Mg(NH_2)_2$ resulted in gaseous products consisting mainly of ammonia. Moreover, the increase in the ball-milling time can effectively suppress the ammonia during the thermal decomposition, and the total amount of hydrogen desorption is about 4.8 wt%.

2.8 Li–Mg–N–H System

Two processes can lead to the formation of $Li_2Mg(NH)_2$. One is via the chemical reaction of $Mg(NH_2)_2$ and 2LiH, and the other is via $2LiNH_2$ and MgH_2. The hydrogenation of $Li_2Mg(NH)_2$ yields $Mg(NH_2)_2 + 2LiH$ Reaction (2.11). This is because $Mg(NH_2)_2$+2LiH is thermodynamically more favored than $2LiNH_2$+ MgH_2.

$$Mg(NH_2)_2 + 2LiH \leftrightarrow Li_2Mg(NH)_2 + 2H_2 \qquad (2.11)$$

$$3Mg(NH_2)_2 + 8LiH \leftrightarrow 4Li_2NH + Mg_3N_2 + 8H_2 \qquad (2.12)$$

It was reported that more than 5 wt% hydrogen can be reversibly stored in $Li_2Mg(NH)_2$ in the temperature range of 100-300°C. The thermodynamic properties are improved considerably compared with those of the binary Li–N–H and Mg–N–H systems. Pressure–composition–temperature (PCT) measurements show that the dehydrogenation of $Mg(NH_2)_2 + 2LiH$ exhibits a pressure plateau region and a slope region. The heat of desorption hydrogen within the pressure plateau is 38.9 kJ/mol H_2. Catalytic modification is important to bring the system a step forward towards practical usage. Altering the molar ratio of $Mg(NH_2)_2$ and LiH will lead to different dehydrogenation products, such as nitride Reaction (2.12). The H-content

can be higher, but the temperature for the hydrogen desorption moves to higher end (Chen *et al.*, 2007).

Chen *et al.* (2006) investigated the structure and hydrogen storage property of ball-milled $LiNH_2/MgH_2$ mixture. The results showed that the initial dehydrogenation reaction between $LiNH_2$ and MgH_2 leads to the formation of a novel Li–Mg–N–H ternary imide, which can be further rehydrogenated to the $Mg(NH)_2$/LiH mixture. Moreover, when operated at 200°C, the material can reversibly store up to 4.3 wt% hydrogen, and 90 % of which can be desorbed within 1 h.

Janot *et al.* (2007) investigated the processes for reversible hydrogen storage in the Li–Mg–N–H system. The results showed that, for $2LiNH_2+MgH_2$, an ammonia release occurred if the first heating was conducted under vacuum, leading to a fast degradation of the material. However, an advantage of adding 2LiH into $Mg(NH_2)_2$ is LiH rapidly reacts with NH_3 and reduces the NH_3 contamination of hydrogen desorption flow. The total amount of 5.0 wt% hydrogen was desorbed after 25 min at 220°C, and exhibited a nice reversibility at 200°C.

Lohstroh and Fichtner (2007) studied the reaction steps in the Li–Mg–N–H systems. The results reported that during the first desorption or intense ball milling, $Mg(NH_2)_2$ was formed as a part of the reversible reaction. $Mg(NH_2)_2$ initially emitted NH_3, which then reacted with LiH to form $LiNH_2$. In the second step, MgNH and either $LiNH_2$ or LiH reacted to form a mixed LiMg–imide phase. The addition of $TiCl_3$ was forced to enhance the milling intensity and therefore lowered the desorption temperature. However, $TiCl_3$ does not have a catalytic effect on the reversible reaction.

Luo (2004) developed a new storage material, which is from the partial substitution of lithium by magnesium. The mixtures between $LiNH_2$ and MgH_2 with 2:1.1 molar ratio were examined. The plateau pressure of the new Mg-substituted system is about 30 bar, and the temperature is 200°C. The amount of hydrogen desorbed is 4.5 wt% and possibly higher because the theoretical capacity is 5.35 wt%. The difference between the theoretical and experimental capacities may result from "isolated islands" of the two solid reactants, and better sample mixing may improve its desorption efficiency.

Luo and Rönnebro (2005) succeeded in destabilizing $LiNH_2$ by partial substitution of lithium by magnesium in the $(LiNH_2 + LiH \leftrightarrow Li_2NH + H_2)$ system with a minimal capacity loss. A mixture of $(2LiNH_2 + MgH_2)$ can be used to reversibly absorb 5.2 wt% hydrogen at pressure of 30 bar at 200°C, which is interesting to observe that the starting material $(2LiNH_2 + MgH_2)$ convert to $(Mg(NH_2)_2 + 2LiH)$ after desorption/re-absorption cycle.

Markmaitree *et al.* (2008a) compared the dehydrogenation kinetics of $(2LiNH_2 + MgH_2)$ and $(LiNH_2 + LiH)$ systems. They found that the $(2LiNH_2 + MgH_2)$ mixture had a higher rate for hydrogen desorption, slower rate for approaching its equilibrium pressure, higher activation energy, and more NH_3 emission than the $(LiNH_2 + LiH)$ mixture. High-energy ball milling can reduce the activation energy of dehydrogenation of both $(2LiNH_2 + MgH_2)$ and $(LiNH_2 + LiH)$ mixtures.

Markmaitree *et al.* (2008b) studied the reaction rates of NH_3 with MgH_2 and LiH. They found that using a two-layered structure containing a top MgH_2 layer and a bottom layer $LiNH_2$. Quantification of the effluent gas composition from the two-layered structure indicated substantial NH_3 emission. In contrast, the study of two-layered structure containing a top LiH layer and a bottom $LiNH_2$ layer revealed that the reaction between LiH and NH_3 is much faster than that between MgH_2 and $LiNH_2$.

Osborn *et al.* (2007) evaluated the hydrogen storage behavior of a 1:1 molar ratio of $LiNH_2 + MgH_2$. They found that the high MgH_2 concentration did not mitigate the issue of NH_3 emission effectively. In addition, the hydrogen storage capacity was lower than that of the $(2LiNH_2 + MgH_2)$ system because of the presence of un-reacted MgH_2 in the $LiNH_2 + MgH_2$ system.

2.9 Li–Al–N–H system

Investigation on the $LiNH_2$–$LiAlH_4$ system revealed that the transition of $[AlH_4]^-$ to $[AlH_6]^{3-}$ is fairly easy in the presence of $LiNH_2$, and a large amount of

hydrogen was desorbed from the system under the ball milling condition. In addition, most hydrogen desorbed during the mechanical ball milling was hard to be recharged back to the material, probably due to thermodynamic reasons. Interestingly, hydrogen can be reversibly stored by Li_3AlN_2, which is the fully dehydrogenated state of the post-milled $2LiNH_2$–$LiAlH_4$ sample Reaction (2.13).

$$2LiNH_2 + LiAlH_4 \rightarrow Li_3AlN_2 + 4H_2 \quad (2.13)$$

$$LiNH_2 + 2LiH + AlN \leftrightarrow Li_3AlN_2 + 2H_2 \quad (2.14)$$

$$4LiNH_2 + 2Li_3AlN_2 \rightarrow Al + 2Li_2NH + 3LiH + \frac{15}{2}H_2 \quad (2.15)$$

Moreover, 5.1 wt% hydrogen can be absorbed and desorbed in a Li_3AlN_2 sample in the temperature range of 100-500°C. The fully hydrogenated sample contains AlN, LiH, and $LiNH_2$, Reaction (2.14) (Chen *et al.*, 2007).

Chen *et al.* (2007) reviewed the metal–N–H systems for the hydrogen storage properties of $LiNH_2 + Li_3AlH_6$. They found a fully reversible reaction between Li_3AlH_6 and $LiNH_2$ with a 1:3 molar ratio. The $Mg(NH_2)_2$–$LiAlH_4$ system has also been investigated, and they reported that the system is more complicated than other binary and ternary systems.

Dolotko *et al.* (2007) studied the mechanochemical transformations in the $Li(Na)AlH_4$–$Li(Na)NH_2$ system with a 1:1 molar ratio. They found that the amount of hydrogen desorption after 30 min of ball-milling was about 6.6 wt%. The mechanism of the overall transformation is Reaction (2.16) with M_3AlH_6 as an intermediate, and M is a metal elements.

$$MAlH_6(s) + MNH_2(s) \rightarrow 2MH(s) + AlN(s) + 2H_2(g) \quad (2.16)$$

In addition, they anticipated that hydrogen would be released mechanochemically at temperatures below the ambient temperature, even though the transformation kinetics may be somewhat slower.

Kojima *et al.* (2006) investigated the temperature-programmed desorption scans of the Li–Al–N–H system, which is the mixture of Li_3AlH_6 and $LiNH_2$ with a 1:2 molar ratio, indicating that a theoretical amount of hydrogen is about 6.9 wt% and it can be released between 97 and 500°C. The desorpion/absorption capacities of the Li–Al–N–H system with a nano-Ni catalyst exhibited 3-4 wt% at 200-300°C, while the capacities of the system without the catalyst are 1-2 wt%.

Nakamori *et al.* (2006) observed the dehydriding reactions of mixed complex hydrides. The results showed that the mixture of $2LiNH_2 + LiAlH_4$ exhibits an endothermic dehydriding reaction and the stability of this reaction can be controlled by introducing new pathways that are producing by mixing.

Xiong *et al.* (2006) investigated chemical reactions between $LiAlH_4$ and $LiNH_2$. The results reported that the kinetic barrier in the transformation from tetrahedral $[AlH_4]^-$ in $LiAlH_4$ to octahedral $[AlH_6]^{3-}$ was easily overcome by mixing with $LiNH_2$ at a 1:1 molar ratio. XRD clearly identified the appearance of Li_3AlH_6 and Al in the milling process. In addition, the total amount of hydrogen desorption was about 8 wt%. They predicted that $[Li_2AlNH]$ is the final product from the desorption reaction.